Multiple Response Prediction and Optimization in Thin-Walled Milling of 6061 Aluminum Alloy

Van Que Nguyen
Faculty of Mechanical Engineering, Hanoi University of Industry, Vietnam
nguyenvanque@haui.edu.vn

Hoang Tien Dung
Faculty of Mechanical Engineering, Hanoi University of Industry, Vietnam
tiendung@haui.edu.vn

Van Thien Nguyen
Personnel and Administrative Department, Hanoi University of Industry, Vietnam
nguyenvanthien@haui.edu.vn

Van Dong Pham
Department of Science and Technology, Hanoi University of Industry, Vietnam
nguyenvanthien@haui.edu.vn

Van Canh Nguyen
Faculty of Mechanical Engineering, Hanoi University of Industry, Vietnam
nguyenvancanh@haui.edu.vn
(corresponding author)

Received: 10 January 2023 | Revised: 4 February 2023 | Accepted: 15 February 2023

ABSTRACT

In this study, the multi-objective optimization method for thin-wall milling of 6061 aluminum alloy is addressed. The technological parameters including the cutting speed V_c, the feed of tooth f_z, and the width of cut a_r are considered input variables, while the manufacturing responses are surface roughness R_a, production rate MRR, and flatness deviation FL. The goal is to find the optimum cutting parameters to minimize R_a and FL and maximize MRR, at the same time. To solve this problem, the desirability function approach was used based on Taguchi orthogonal array. Twenty-seven experiments were conducted and the measured data were collected. The mathematical regression models for responses *Ra*, MRR, and FL were then generated and evaluated by using the analysis of variance method. Then, the multiple objective optimization problems were solved by using the desirability function approach. The optimum cutting parameters set are V_c=120m/min, f_z=0.06mm, and a_r=0.13131mm, corresponding to *Ra*=0.1613μm, MRR=17197.45cm^3/min, and FL=0.0995mm.

Keywords-thin-walled milling; multiple objective optimization; desirable function approach; Taguchi method; 6061 aluminum alloy

I. INTRODUCTION

The 6061 alloy is an important product line in aluminum manufactured products [1]. Aluminum and its alloys rank second (after steel) in use as structural metals [2], due to properties that make them suitable for many different uses [3]. Some of the important properties of 6061 alloy are its light weight, high strength, good chemical corrosion resistance, and good weldability [4]. Therefore, 6061 alloy is often used in the transportation industry (e.g. in auto parts, motorcycles, cycle frames, and motorcycle frames) and especially in the marine or aerospace industry [5]. The development of the aviation

industry has led to an increasing demand for aluminum alloy machining, in which the milling of thin-walled parts plays a particularly important role [6]. However, the manufacturing of thin-walled parts is complicated by the possibility of deformation during the machining process [7]. Thin-walled products are often difficult to cut due to the complex dynamics involved. During the cutting process, the cutting dynamics for the products varies however it is invariant for the machine tool [8]. On another hand, permanent deformation of the structure can occur and this can cause a proportion of rejected products [9].

In the demand of the growing global market for aluminum alloy thin-walled products, there are several studies focused on optimizing the structure to improve the surface roughness, the load capacity, and the durability of the thin-walled components by reducing deformation and vibration during the cutting process [7]. Many studies have been carried out to improve the economic and technical efficiency of thin-walled processing. Authors in [10] developed an analytical approach to investigate the dynamic chip thickness variation in the thin-walled milling process. A general model of the removal volume is calculated by considering the individual axial depth of cut, the radial depth of cut, and the circumferential cross-section of the tool radius contact for each tool step performed. Authors in [6] presented a technique to improve the surface quality and production rate in the thin-walled milling process. The results show that double-side milling leads to reduce about 50% in cutting time and a decline in the surface roughness and flatness deviation of the milling products, simultaneously. The quality of thin-walled products when machined can also be improved by selecting and using the right jigs and fixtures [11]. Finding suitable cutting parameters can also reduce vibration, thereby reducing deformation during milling. This can be solved through experimentation [12, 13], or mathematical modelling [14]. Authors in [8] present a methodology of performing the optimization of the entire cutting process for thin-walled parts based on the relatively changing kinematics of the machining system. According to the comparison between the dynamics of the machine tool and the variable thickness part, the critical thickness is investigated by an iterative algorithm. This method can be used for many other machining processes.

There are many other studies on machining thin-walled parts in general, and aluminum alloys in particular. These studies can be applied to improve the quality of processed products in practice. However, due to the increasing competitive pressure from the global market, the manufacturers not only have to improve the quality of processing but at the same time have to increase machining productivity and tool life. Those are scientific multi-objective optimization problems and Multiple Criteria Decision-Making (MCDM) methods such as the Technique for Order of Preference by Similarity to Ideal Solution (TOPSIS) and Multi-Objective Optimization on the basis of Ratio Analysis (MOORA) have been introduced to face them [15-19]. They are often applied due to their simplicity. However, these methods have a common disadvantage, which is the optimal value set is one of the experimental values. This means that these techniques select one of the data sets that have been used, and in many cases, they are not the best [18-20].

With the development of computers, many new algorithms have been researched and applied, e.g. ANFIS [21], Desirability Function Approach (DFA) [22], etc. Many publications have demonstrated the effectiveness of these methods in comparison with MCDM. In this study, DFA and Minitab computed software were applied to solve the multi-objective optimization problem at hand. The research aims to find the optimal cutting parameters set to simultaneously maximize the machining productivity MRR, and minimize the roughness R_a and flatness deviation FL.

A. MATERIALS AND METHODS

B. 6061 Aluminum Alloy

As mentioned above, 6061 Aluminum Alloy was selected because it is largely used. All the specimen workpieces were milled with dimensions of $100\times50\times10mm^3$. The chemical composition and mechanical properties of the workpieces are shown in Tables I and II [23]. The experiments were conducted on a DMU50 CNC Machine. To perform thin-walled milling operations, a 3-flute square namely YG ALU - CUTTER E5D70100 (15329040K) was used (Figure 1). The Taguchi orthogonal array was applied to reduce the number of experiments but still ensure reliability in the predictive analysis, with the number of input variables being 3, the number of levels for each variable being 3, and the number of experiments to be performed being 27. The values of the input variables corresponding to the levels are depicted in Table III. The range of the cutting parameters is chosen based on the cutting tool manufacturer's recommendations.

TABLE I. CHEMICAL COMPOSITION OF 6061 ALLOY

Al (%)	Mg (%)	Si (%)	Cu (%)	Cr (%)	Others (%)
97.9	1	0.60	0.28	0.20	0.02

TABLE II. THE MECHANICAL PROPERTIES OF 6061 ALLOY

Tensile strength	310MPa
Yield strength	276MPa
Shear strength	207MPa
Fatigue strength	96.5MPa
Elastic modulus	68.9GPa
Poisson's ratio	0.33
Elongation	12-17%
Hardness	95 HB

TABLE III. INPUT VARIABLE LEVELS

Parameters	Symbol	Unit	Level		
			-1	0	1
Cutting speed	V_c	m/min	120	150	180
Feed rate	f_z	mm/tooth	0.04	0.05	0.06
Width of cut	a_r	mm	0.8	1.0	1.2

C. Experimental data acquisition

The experimental set up is shown in Figure 2. In this work, 3 thin-walled cutting responses, including the surface roughness *Ra*, material removal rate MRR, and flatness deviation FL are optimized simultaneously by applying the Desirable Function Approach (DFA). Based on the EN ISO 4287 standard, surface roughness R_a is calculated by:

$$R_{ax} = \frac{R_{ax1}+R_{ax2}+R_{ax3}+R_{ax4}+R_{ax5}}{5} \quad (1)$$

$$R_{ay} = \frac{R_{ay1}+R_{ay2}+R_{ay3}+R_{ay4}+R_{ay5}}{5} \quad (2)$$

$$R_a = \frac{R_{ax}+R_{ay}}{2} \quad (3)$$

where R_{ax} is the arithmetical mean roughness in the x-direction and R_{ay} is the mean roughness depth in the y-direction.

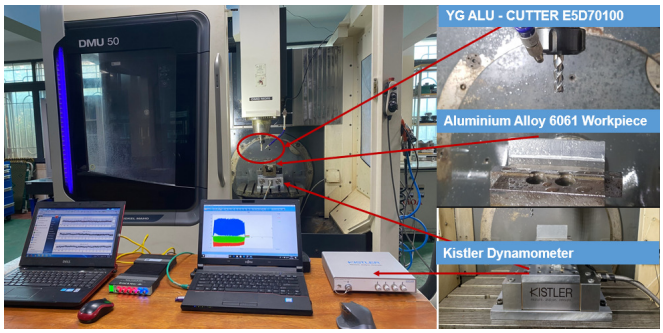

Fig. 1. The experimental setup.

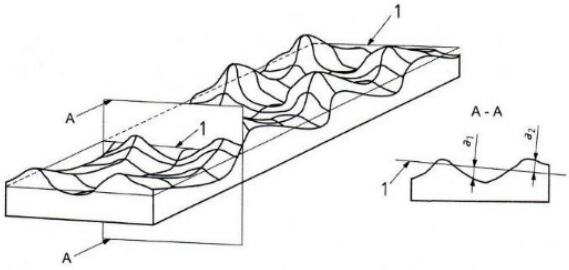

Fig. 2. a_1: Negative local flatness deviation, a_2: Positive local flatness deviation, 1: least squares reference plane (STN P CEN ISO/TS 12781-1: 2008).

(a)

(b)

Fig. 3. Measurement systems. (a) Renishaw Equator 300 CMM - High-Speed Comparative Gauge System, (b) Non-contact flatness deviation measurement system.

TABLE IV. EXPERIMENTAL RESULTS

Run	V_c m/min	f_z mm/	a_r mm	R_a µm	MRR mm^3/min	FL mm
1	120	0.04	0.8	0.228	8025.48	-0.031
2	120	0.05	1	0.128	14331.21	-0.060
3	120	0.06	1.2	0.152	20636.94	-0.044
4	150	0.04	0.8	0.294	10031.85	0.100
5	150	0.05	1	0.274	17914.01	0.063
6	150	0.06	1.2	0.345	25796.18	0.131
7	180	0.04	0.8	0.157	11369.43	-0.015
8	180	0.05	1	0.170	20302.55	-0.045
9	180	0.06	1.2	0.271	29235.67	0.039
10	180	0.04	1	0.150	16242.04	0.050
11	180	0.05	1.2	0.205	24363.06	0.085
12	180	0.06	0.8	0.206	17054.14	0.029
13	120	0.04	1	0.190	11464.97	0.033
14	120	0.05	1.2	0.172	17197.45	0.048
15	120	0.06	0.8	0.170	12038.22	-0.023
16	150	0.04	1	0.275	14331.21	0.085
17	150	0.05	1.2	0.300	21496.82	0.192
18	150	0.06	0.8	0.300	15047.77	0.130
19	150	0.04	1.2	0.292	17197.45	0.368
20	150	0.05	0.8	0.279	12539.81	0.058
21	150	0.06	1	0.309	21496.82	0.055
22	180	0.04	1.2	0.175	19490.45	0.253
23	180	0.05	0.8	0.163	14211.78	-0.050
24	180	0.06	1	0.227	24363.06	-0.046
25	120	0.04	1.2	0.196	13757.96	0.234
26	120	0.05	0.8	0.181	10031.85	-0.084
27	120	0.06	1	0.161	17197.45	-0.099

In this experiment, the surface roughness value of each experiment was measured 3 times on a Renishaw Equator 300 CMM - High-Speed Comparative Gauge System (Figure 3) according to the EN ISO 4287 standard. The flatness deviation (FL, mm) is measured using a non-contact measurement system (Figure 3). According to STN P CEN ISO/TS 12781-2: 2008 standard, the flatness zone was divided into negative and positive (Figure 2) local zones based on the least squares reference plane, which is a plane such that the sum of the squares of the local flatness deviations is minimum. The measured results are summarized in Table IV.

The Material Removal Rate-MRR (mm^3/min) of each experiment is calculated by:

$$MRR = a_p \times a_e \times N \times S \times f_z \quad (4)$$

where a_p is the depth of cut (mm). In this experimental work, a_p=10mm for all runs. a_r is the width of cut (mm), N is the number of cut flutes (N=3), S is the spindle speed (rpm), and f_z is the feed of tooth (mm/tooth).

The matrix of the experiment design with the input factors and the response data is presented in Table IV. These data were utilized to develop the regression models for R_a, MRR, and FL.

D. The Optimization Problem

The machining parameters, i.e. cutting speed V_c, feed rate f_z, and width of cut a_r, and their corresponding levels are listed in Table III. The target of this research is to decrease the flatness deviation FL and improve the MRR concerning the predefined R_a. Consequently, the optimizing issue can be described as (5):

Find X={V_c, f_z, a_r} to minimize {R_a; FL}, and maximize MRR subjected to $120 \le V_c \le 180$ (m/min); $0.04 \le f_z \le 0.06$ (mm/tooth) and $0.8 \le a_r \le 1.2$ (mm) (5)

To solve this multi-object problem, the DFA was adopted. The desirability package contains S3 classes to optimize multiple variables simultaneously using the DFA of Harrington [24-26] (1965) with the functions described in [24, 25]. Basically, the method is to translate the functions to a common scale ([0, 1]), combine them using the geometric mean and optimize the overall index. For each function R, an individual "desirability" function is constructed to be high when $f_r(x)$ is at the desired level (such as maximum, minimum, or target) and low when the $f_r(x)$ is at an unwanted level value. Authors in [27] proposed three forms of these functions, corresponding to the type of optimization goal. To maximize $f_r(x)$, d_r^{max}, d_r^{mmin} are obtained for maximization and minimization purposes, while d_r^{target} represents for the best solution.

$$d_r^{max} = \begin{cases} 0 & \text{if } f_r(x) < A \\ \left(\frac{f_r(x)-A}{B-A}\right)^S & \text{if } A \le f_r(x) \le B \\ 1 & \text{if } f_r(x) > B \end{cases} \quad (6)$$

$$d_r^{min} = \begin{cases} 0 & \text{if } f_r(x) > B \\ \left(\frac{f_r(x)-B}{A-B}\right)^S & \text{if } A \le f_r(x) \le B \\ 1 & \text{if } f_r(x) < A \end{cases} \quad (7)$$

$$d_r^{target} = \begin{cases} \left(\frac{f_r(x)-A}{t_0-A}\right)^{S1} & \text{if } A \le f_r(x) \le t_0 \\ \left(\frac{f_r(x)-B}{t_0-B}\right)^{S2} & \text{if } t_0 \le f_r(x) \le B \\ 0 & \text{otherwise} \end{cases} \quad (8)$$

II. RESULTS AND DISCUSSION

A. Regression models

The regression models for R_a, MRR, and FL were generated using Minitab Software. Equations (9)-(11) show the fully developed regression models.

$$R_a = -1.609 + 0.04550V_c - 38.20f_z - 1.066a_r - 0.000188V_c^2 + 173.9f_z^2 + 0.2767a_r^2 + 0.1307V_cf_z + 0.002964V_c.a_r + 2.53a_rf_z \quad (9)$$

$$\text{MRR} = 16932 - 115.4V_c - 338641f_z - 17516a_r - 0.0000V_c^2 + 0.0000f_z^2 + 0.0000a_r^2 + 2309V_cf_z + 119.43V_c.a_r + 340318a_rf_z \quad (10)$$

$$FL = -2.390 + 0.05237V_c - 33.26f_z - 1.267a_r - 0.000188V_c^2 + 465.7f_z^2 + 1.470a_r^2 + 0.0490V_cf_z + 0.00407V_c.a_r - 26.42a_rf_z \quad (11)$$

To assess the adequacy of these models, analysis of variance (ANOVA) was adopted. The ANOVA was conducted with 95% of confidence and 5% significance. The ANOVA results for the predictive models are presented in Tables V-VII.

The coefficients of mathematical regression models, including "R^2", "adjusted R^2," and "predicted R^2," reveal the accuracy of the developed models. In this work, the values of "R^2", "adjusted R^2," and "predicted R^2," for R_a, MRR, and FL the are fluctuated in the range of [96.66%, 99.93%], [94.89%, 99.89%], and [89.78%, 99.76%] mean a good fitting between the experimental and the predicted values. Hence, it is concluded that the developed models of R_a, MRR, and FL can be used for predicting the optimal process parameters.

TABLE V. ANOVA FOR THE PREDICTIVE MODELS OF R_a

Term	DF	Adj SS	Adj MS	F-Value	P-Value
Regression	9	0.102879	0.011431	54.64	0
V_c	1	0.039154	0.039154	187.14	0
f_z	1	0.006102	0.006102	29.16	0
a_r	1	0.003528	0.003528	16.86	0.001
V_c*V_c	1	0.079044	0.079044	377.8	0
f_z*f_z	1	0.001814	0.001814	8.67	0.009
a_r*a_r	1	0.001452	0.001452	6.94	0.017
V_c*f_z	1	0.012573	0.012573	60.09	0
V_c*a_r	1	0.004044	0.004044	19.33	0
f_z*a_r	1	0.000413	0.000413	1.97	0.178
Error	17	0.003557	0.000209		
Total	26	0.106436			

"R^2"=96.66%, "Adjusted R^2"=94.89% and "predicted R^2"=89.78%

TABLE VI. ANOVA FOR THE PREDICTIVE MODELS OF MRR

Term	DF	Adj SS	Adj MS	F-Value	P-Value
Regression	9	728005304	80889478	2553.25	0
V_c	1	199266	199266	6.29	0.023
f_z	1	720212	720212	22.73	0
a_r	1	1209228	1209228	38.17	0
V_c*V_c	1	1999162	1999162	63.1	0
f_z*f_z	1	0	0	0	1
a_r*a_r	1	4602114	4602114	145.26	0
V_c*f_z	1	3998324	3998324	126.21	0
V_c*a_r	1	6685664	6685664	211.03	0
f_z*a_r	1	9204227	9204227	290.53	0
Error	17	538577	31681		
Total	26	728543881			

"R^2"=99.93%, "Adjusted R^2"=99.89% and "predicted R^2"=99.76%

TABLE VII. ANOVA FOR THE PREDICTIVE MODELS OF FL

Term	DF	Adj SS	Adj MS	F-Value	P-Value
Regression	9	0.315328	0.035036	97.42	0
V_c	1	0.058999	0.058999	164.04	0
f_z	1	0.002633	0.002633	7.32	0.015
a_r	1	0.006217	0.006217	17.28	0.001
V_c*V_c	1	0.08127	0.08127	225.96	0
f_z*f_z	1	0.013011	0.013011	36.17	0
a_r*a_r	1	0.03372	0.03372	93.75	0
V_c*f_z	1	0.001546	0.001546	4.3	0.054
V_c*a_r	1	0.000111	0.000111	0.31	0.585
f_z*a_r	1	0.054928	0.054928	152.72	0
Error	17	0.006114	0.00036		
Total	26	0.321442			

"R^2"= 98.10%, "Adjusted R^2"=97.09% and "predicted R^2"=96.09%

B. Multiple Objective Optimization results

As mentioned above, the DFA was adopted for solving the multiple objective problem (Figure 4). The Composite Desire Values (D) corresponding to 27 experiments were computed using the Minitab 19 software with the constrain from (5). The results are shown in Table VIII.

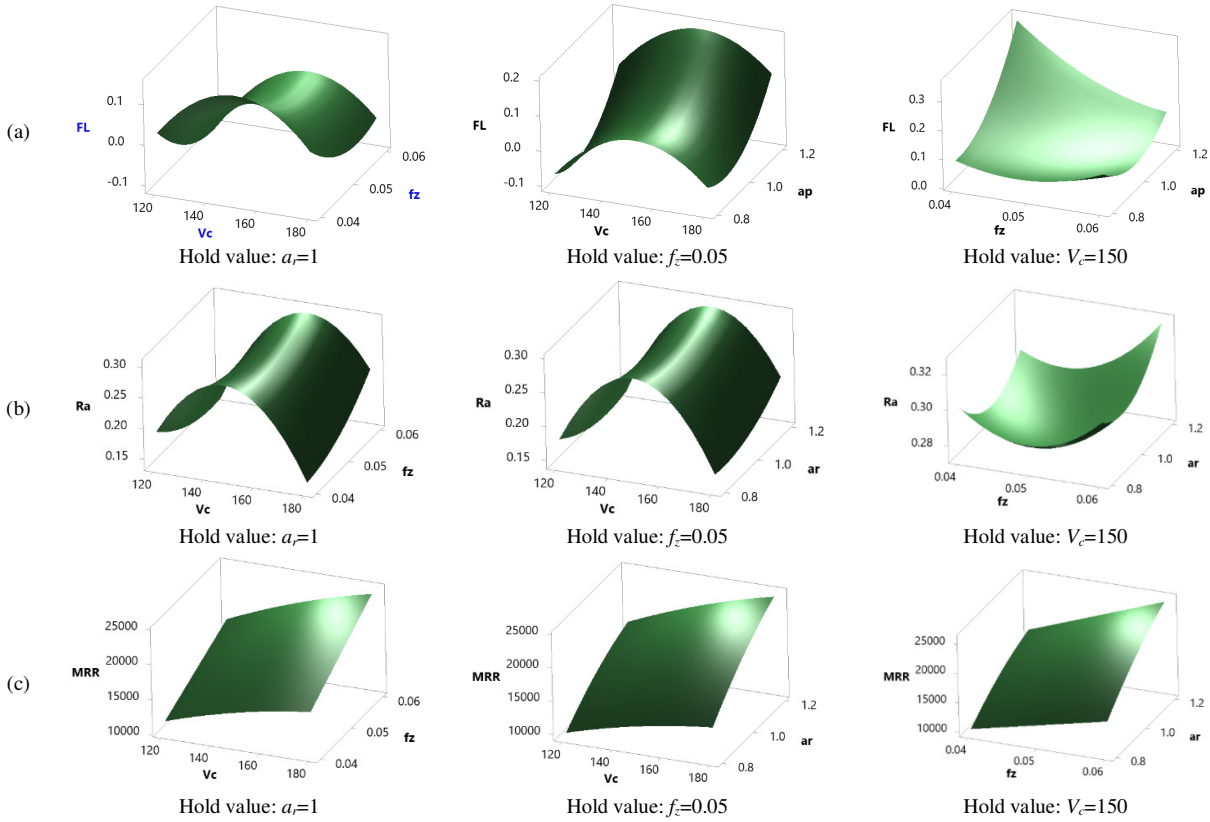

Fig. 4. Surface plot of (a) FL, (b) R_a, (c) MRR vs V_c, f_z, a_r.

TABLE VIII. COMPOSITE DESIRABILITY VALUE (D)

Solution	Vc	fz	ar	FL fit	MRR fit	R_a Fit	D
1	**120**	**0.060**	**1.131**	**-0.07**	**19829.00**	**0.145**	**0.769**
2	120	0.060	1.180	-0.04	20596.40	0.149	0.763
3	120	0.060	1.199	-0.03	20866.70	0.151	0.758
4	120	0.060	1.200	-0.03	20879.10	0.151	0.757
5	180	0.058	1.052	-0.04	24881.10	0.223	0.718
6	180	0.060	1.034	-0.04	25165.70	0.233	0.699
7	180	0.060	1.012	-0.04	24533.80	0.230	0.698
8	180	0.060	1.137	0.00	27867.10	0.255	0.662

The higher the value of D, the more optimal the experiment is. In this study, the optimal parameter set V_c = 120m/min, f_z = 0.06mm, a_r = 1.13131mm correspond to R_a = 0.144601µm, MRR = 19829cm^3/min, and FL = -0.00699460mm.

Comparing the optimization results with the resurged results shown in Table I, it is easy to see that the optimization results are quite close to the experiment number 27. However, the difference is that the predicted a_r value is larger than the selected a_r value, at 1mm and 1.131mm, respectively. This increase in the width of the cut led to an increase in production rate by about 15.30%, from 17197.45 to 19829cm^3/min. At the same time, the surface roughness value R_a decreased by 13.10%, from 0.1613 to 0.1446µm and the FL also decreased by -0.07mm, a decrease of 29.65%.

The results of this study show the advantages of DFA in comparison with DCDM. The disadvantage of DCDM is that the optimal parameter set is calculated, ranked, and selected from one of the experimental runs, in this case, experiment number 27. With the DFA method, the optimal parameters do not necessarily coincide with the selected parameters. The comparison results are clearly depicted in Table IX.

TABLE IX. OPTIMIZATION RESULT COMPARISON

	Cutting parameters			Responses		
	Vc **(m/min)**	f_z **(mm)**	a_r **(mm)**	R_a **(µm)**	**MRR (cm3/min)**	**FL (mm)**
Actual value	120	0.06	1	0.1613	17197.45	-0.0995
Predicted value	120	0.060	1.131	0.145	19829.00	-0.07
Comparison				↓13.10%	↑15.30%	↓29.65%

III. CONCLUSION

Due to the increasing competitive pressure from the global market, the need to maintain or increase product quality while simultaneously increasing productivity is important. This is a multi-objective optimization problem. In this article, the multiple objective optimization issue in thin-walled milling of 6061 aluminum alloy for reducing flatness deviation FL and surface roughness R_a while improving production rate MMR simultaneously, has been addressed. Predictive mathematical regression models of the three responses have been developed to model the highly non-linear relations between the cutting parameters (i.e. V_c, f_z, and a_r) and the machining responses. The Desirability Function Approach (DFA) was employed to

generate the optimum parameters. The main results of this work can be concluded, as follows:

The "R^2", "adjust-R^2" and "predicted-R^2" of R_a, MRR, and FL fluctuated around 90-99%, illustrating the good relationship between cutting parameters and response. Hence, these mathematical regression models could be applied in the actual manufacturing process to predict the cutting parameters set corresponding to the desired response. The obtained optimal cutting parameters set of thin-walled milling of 6061 aluminum alloy processes is (V_c=120m/min, f_z=0.06mm, and a_r=1.13434mm), corresponding to the R_a, MRR, and FL values of 0.14269µm, 19614.6mm^3/min, and -0.0653mm, respectively.

The findings in this research work can contribute to a broader understanding of aluminum alloy thin-walled milling and can be extended to research with other materials and machining processes. In future works, other cutting parameters such as tool nose radius, tool coaching material, lubrication method, number of inserts, number of flutes, and other responses including cutting force, cutting variation, tool wear, and tool life will be taken into consideration.

ACKNOWLEDGMENT

This research is supported by the Hanoi University of Industry (HaUI).

REFERENCES

[1] D. Carou and J. P. Davis, Eds., *Machining of Light Alloys: Aluminum, Titanium, and Magnesium*, 1st ed. Boca Raton: CRC Press, 2018.

[2] J. R. Davis, Ed., *Alloying: Understanding the Basics - ASM International*. ASM International, 2001.

[3] W. Rajhi, "Numerical Simulation of Damage on Warm Deep Drawing of Al 6061-T6 Aluminium Alloy," *Engineering, Technology & Applied Science Research*, vol. 9, no. 5, pp. 4830–4834, Oct. 2019, https://doi.org/10.48084/etasr.3148.

[4] J. P. Davis, Ed., *Mechatronics and Manufacturing Engineering: Research and Development*, 1st ed. Woodhead Publishing, 2016.

[5] D. X. Biên, N. V. Công, Đ. Đ. Mạnh, N. V. Đức, N. T. Kiên, and Đ. V. Dưỡng, "Nghiên cứu ảnh hưởng của chiến lược chạy dao tới chất lượng gia công các dạng thành mỏng khi phay cao tốc hợp kim nhôm AL6061," *Tạp Chí Cơ khí Việt Nam*, vol. 4, pp. 33–39, 2015.

[6] M. K. Mejbel, I. T. Abdullah, and N. K. Taieh, "Thin Wall Manufacturing Improvement using Novel Simultaneous Double-Sided Cutter Milling Technique," *International Journal of Automotive and Mechanical Engineering*, vol. 19, no. 1, pp. 9519–9529, Mar. 2022, https://doi.org/10.15282/ijame.19.1.2022.15.0734.

[7] I. Del Sol, A. Rivero, L. N. López de Lacalle, and A. J. Gamez, "Thin-Wall Machining of Light Alloys: A Review of Models and Industrial Approaches," *Materials*, vol. 12, no. 12, Jan. 2019, Art. no. 2012, https://doi.org/10.3390/ma12122012.

[8] Y. Tang, J. Zhang, J. Yin, L. Bai, H. Zhang, and W. Zhao, "Relative Varying Dynamics Based Whole Cutting Process Optimization for Thin-walled Parts," *Chinese Journal of Mechanical Engineering*, vol. 35, no. 1, Dec. 2022, Art. no. 145, https://doi.org/10.1186/s10033-022-00815-z.

[9] S. Borojevic, D. Lukic, M. Milosevic, J. Vukman, and D. Kramar, "Optimization of process parameters for machining of Al 7075 thin-walled structures," *Advances in Production Engineering & Management*, vol. 13, no. 2, pp. 125–135, Jun. 2018, https://doi.org/10.14743/apem2018.2.278.

[10] M. Masmali and P. Mathew, "An Analytical Approach for Machining Thin-walled Workpieces," *Procedia CIRP*, vol. 58, pp. 187–192, Jan. 2017, https://doi.org/10.1016/j.procir.2017.03.186.

[11] K. Mori and A. Matsubara, "Estimation of supporting fixture receptance for thin-walled milling," *CIRP Annals*, vol. 71, no. 1, pp. 333–336, Jan. 2022, https://doi.org/10.1016/j.cirp.2022.04.038.

[12] B. Li, X. Jiang, J. Yang, and S. Y. Liang, "Effects of depth of cut on the redistribution of residual stress and distortion during the milling of thin-walled part," *Journal of Materials Processing Technology*, vol. 216, pp. 223–233, Feb. 2015, https://doi.org/10.1016/j.jmatprotec.2014.09.016.

[13] S. Ren, X. Long, and G. Meng, "Dynamics and stability of milling thin walled pocket structure," *Journal of Sound and Vibration*, vol. 429, pp. 325–347, Sep. 2018, https://doi.org/10.1016/j.jsv.2018.05.028.

[14] Y. Sun and S. Jiang, "Predictive modeling of chatter stability considering force-induced deformation effect in milling thin-walled parts," *International Journal of Machine Tools and Manufacture*, vol. 135, pp. 38–52, Dec. 2018, https://doi.org/10.1016/j.ijmachtools.2018.08.003.

[15] N. M. M. Reddy and P. K. Chaganti, "Investigating Optimum SiO2 Nanolubrication During Turning of AISI 420 SS," *Engineering, Technology & Applied Science Research*, vol. 9, no. 1, pp. 3822–3825, Feb. 2019, https://doi.org/10.48084/etasr.2537.

[16] V. K. B. Ponnam and K. Swarnasri, "Multi-Objective Optimal Allocation of Electric Vehicle Charging Stations and Distributed Generators in Radial Distribution Systems using Metaheuristic Optimization Algorithms," *Engineering, Technology & Applied Science Research*, vol. 10, no. 3, pp. 5837–5844, Jun. 2020, https://doi.org/10.48084/etasr.3517.

[17] A. K. Kiamehr, A. Azar, and M. D. Nayeri, "A Multi-Objective Optimization Model for Designing Business Portfolio in the Oil Industry," *Engineering, Technology & Applied Science Research*, vol. 8, no. 6, pp. 3657–3667, Dec. 2018, https://doi.org/10.48084/etasr.2023.

[18] V. C. Nguyen, T. D. Nguyen, and D. H. Tien, "Cutting Parameter Optimization in Finishing Milling of Ti-6Al-4V Titanium Alloy under MQL Condition using TOPSIS and ANOVA Analysis," *Engineering, Technology & Applied Science Research*, vol. 11, no. 1, pp. 6775–6780, Feb. 2021, https://doi.org/10.48084/etasr.4015.

[19] N. Benmoussa, A. Elyamami, K. Mansouri, M. Qbadou, and E. Illoussamen, "A Multi-Criteria Decision Making Approach for Enhancing University Accreditation Process," *Engineering, Technology & Applied Science Research*, vol. 9, no. 1, pp. 3726–3733, Feb. 2019, https://doi.org/10.48084/etasr.2352.

[20] T. Do Duc, N. Nguyen Ba, C. Nguyen Van, T. Nguyen Nhu, and D. Hoang Tien, "Surface Roughness Prediction in CNC Hole Turning of 3X13 Steel using Support Vector Machine Algorithm," *Tribology in Industry*, vol. 42, no. 4, pp. 597–607, Dec. 2020, https://doi.org/10.24874/ti.940.08.20.11.

[21] D. Nguyen, S. Yin, Q. Tang, P. X. Son, and L. A. Duc, "Online monitoring of surface roughness and grinding wheel wear when grinding Ti-6Al-4V titanium alloy using ANFIS-GPR hybrid algorithm and Taguchi analysis," *Precision Engineering*, vol. 55, pp. 275–292, Jan. 2019, https://doi.org/10.1016/j.precisioneng.2018.09.018.

[22] S. V. Alagarsamy, M. Ravichandran, and H. Saravanan, "Development of Mathematical Model for Predicting the Electric Erosion Behavior of TiO2 Filled Al-Zn-Mg-Cu (AA7075) Alloy Composite Using RSM-DFA Method," *Journal of Advanced Manufacturing Systems*, vol. 20, no. 1, pp. 1–26, Mar. 2021, https://doi.org/10.1142/S0219686721500013.

[23] J. R. Davis, *ASM Specialty Handbook: Aluminum and Aluminum Alloys*. ASM International, 1993.

[24] M. Kuhn, "The desirability Package," Sep. 2016.

[25] A. Dean, M. Morris, J. Stufken, and D. Bingham, Eds., *Handbook of Design and Analysis of Experiments*. Boka Raton, FL, USA: CRC Press, 2015.

[26] K. M. Senthilkumar, R. Thirumalai, T. A. Selvam, A. Natarajan, and T. Ganesan, "Multi objective optimization in machining of Inconel 718 using taguchi method," *Materials Today: Proceedings*, vol. 37, pp. 3466–3470, Jan. 2021, https://doi.org/10.1016/j.matpr.2020.09.333.

[27] G. Derringer and R. Suich, "Simultaneous Optimization of Several Response Variables," *Journal of Quality Technology*, vol. 12, no. 4, pp. 214–219, Oct. 1980, https://doi.org/10.1080/00224065.1980.11980968.